Neural Control of Fast Nonlinear Systems— Application to a Turbocharged SI Engine With VCT — Source link ↗

G. Colin, Y. Chamaillard, Gérard Bloch, Gilles Corde

Institutions: Nancy-Université, Institut Français

Related papers:

- Internal combustion engine fundamentals

- Modelling and control of the air system of a turbocharged gasoline engine

- Predictive Control With Constraints

- Introduction to Modeling and Control of Internal Combustion Engine Systems

- Downsizing a Gasoline Engine Using Turbocharging with Direct Injection

Neural control of fast nonlinear systems - Application to a turbocharged SI engine with VCT

Guillaume Colin, Yann Chamaillard, Gérard Bloch, Gilles Corde

Neural control of fast nonlinear systems Application to a turbocharged SI engine with VCT

Guillaume Colin, Yann Chamaillard, Gérard Bloch, and Gilles Corde

Abstract— Nowadays, (engine) downsizing using turbocharging appears as a major way in reducing fuel consumption and pollutant emissions of Spark Ignition (SI) engines. In this context, an efficient control of the air actuators (throttle, Turbo Wastegate and Variable Camshaft Timing (VCT)) is needed for engine torque control. This work proposes a nonlinear model-based control scheme which combines separate, but coordinated, control modules. Theses modules are based on different control strategies: Internal Model Control (IMC), Model Predictive Control (MPC), and optimal control. It is shown how neural models can be used at different levels and included in the control modules to replace physical models, which are too complex to be on-line embedded, or to estimate non measured variables. The results obtained from two different test benches show the real time applicability and good control performance of the proposed methods.

Index Terms— Neural Networks, Nonlinear Control, Engine Control, Internal Model Control, Model Predictive Control.

I. INTRODUCTION

More stringent standards are being imposed to reduce fuel consumption and pollutant emissions for Spark Ignited (SI) engines. Modern automobile engines must therefore satisfy the challenging, and often conflicting, goals of minimizing pollutant emissions and fuel consumption while satisfying driving performance over a wide range of operating conditions. A solution for reducing fuel consumption and thus carbon dioxide (CO_2) emissions is to improve the efficiency of the engine and, to this end, several solutions have been developed: lean combustion, variable valve actuation, downsizing, hybrid engine, fuel cells, etc. . .

Downsizing is the use of a smaller capacity engine operating at higher specific engine loads, i.e. at better efficiency points. Without having to completely change the engine structure, like in hybrid or fuel cell approaches, downsizing appears as a major way for reducing fuel consumption while maintaining the advantage of low emission capability of three-way catalytic systems and combining several well known technologies [1]. A well-adapted turbocharger seems to be the best solution to feed the engine with the aim of reducing fuel consumption. Unfortunately, turbocharger inertia involves a long torque

time response [1]. This problem can be solved by combining turbocharger and Variable Camshaft Timing (VCT) for air scavenging from the intake to the exhaust. Moreover, VCT decreases pollutants emission especially nitrogen oxides (NO_x).

With the multiplication of complex actuators, advanced engine control is necessary to obtain an efficient torque control [2]. This notably includes the control of the ignition coils, fuel injectors and air actuators. The air actuator controllers generally used are PID controllers which are difficult to tune. Moreover, they often produce overshooting and bad set point tracking because of the system nonlinearities. Only model-based control can enhance engine torque control.

Several common characteristics can be found in engine control problems. First of all, the descriptive models are dynamic and nonlinear. They require a vast amount of work to be determined, particularly to fix the parameters specific to each engine type ("mapping"). For control, a sampling period variable with the engine speed (very short in the worst case) must be considered. The actuators present strong saturations. Moreover, many internal state variables are not measured, partly because of the physical impossibility of measuring and the difficulties in justifying the cost of setting up additional sensors. On a higher level, the control must be multi-objective, in order to satisfy contradictory constraints (performance, comfort, consumption, pollution). Lastly, the control must be implemented on on-board computers (Electronic Control Units, ECU), whose computing power is increasing, but remains limited.

In addition, artificial neural networks have been the focus of a great deal of attention during the last two decades, due to their capabilities to solve nonlinear problems by learning from data. Although a broad range of neural network architectures can be found, MultiLayer Perceptrons (MLP) and Radial Basis Function Networks (RBFN) are the most popular neural models, particularly for system modeling and identification [3]. The universal approximation and flexibility properties of such models enable the development of modeling approaches, and then control and diagnosis schemes, which are independent of the specificities of the considered systems. They allow construction of nonlinear global models, static or dynamic. Moreover, neural models can be easily and generically differentiated so that a linear model can be extracted at each sample time and used for the control design. Neural systems can then replace a combination of control algorithms and look-up tables used in traditional control systems and reduce the development

G. Colin and Y. Chamaillard are with the Laboratoire de Mécanique et d'Energétique (LME, EA 1206), 8 rue Léonard de Vinci, 45072 Orléans Cedex 2, France.

G. Bloch is with the Centre de Recherche en Automatique de Nancy (CRAN - UMR 7039), Nancy-University, CNRS, CRAN-ESSTIN, rue Jean Lamour, 54519 Vandoeuvre les Nancy, France. Corresponding author: gerard.bloch@esstin.uhp-nancy.fr

G. Corde is with the Institut Francais du Pétrole (IFP), Avenue du bois Préau, 92852 Rueil Malmaison, France.

effort and expertise for the control system calibration of new engines. Neural networks can be used as observers or software sensors, in the context of a low number of measured variables. They enable the diagnosis of complex malfunctions by classifiers determined from a base of signatures. For the control synthesis, high frequency models (or simulators) can be used. They are very complex and accurate but cannot be embedded. As physical models are too complex, black-box solutions as neural networks become attractive techniques for engine modeling and control. Moreover, the learning processes can be achieved on simulators and/or engine test benches. Recurrent networks, i.e. including internal loops, were used as system direct models and as controllers determined by specialized training for various automobile applications: ABS, active suspension systems and idle control [4]. Neural networks were used also for AFR regulation [5] and could model a variable valve timing engine [6].

As a parsimonious and flexible universal approximator, the perceptron with one hidden layer and with a linear output unit is used here. Its form is given, for a single output f_{nn}, by:

$$f_{nn} = \sum_{k=1}^{n} w_k^2 \; g \left(\sum_{j=1}^{p} w_{kj}^1 \varphi_j + b_k^1 \right) + b^2 \qquad (1)$$

where the φ_j are the p inputs of the network (or regressors), and w_{kj}^1, b_k^1 are weights and biases (or parameters) of n hidden neurons (or nodes), the activation function g is a sigmoid function (often the hyperbolic tangent $g(x) = 2/(1 + e^{-2x}) - 1$), and w_k^2, b^2 are the weights and bias of the output neuron. The neural structure can contain direct linear links between the inputs and output nodes to accurately model mixed linear and nonlinear relationships.

In addition, this neural model can be easily differentiated with respect to the inputs, which is interesting when linearizing around an operating point:

$$\frac{\partial f_{nn}}{\partial \varphi_i} = \sum_{k=1}^{n} w_k^2 w_{ki}^1 \; \dot{g} \left(\sum_{j=1}^{p} w_{kj}^1 \varphi_j + b_k^1 \right) \qquad (2)$$

where $\dot{g}$ is the derivative of g with respect to its inputs.

Thus, for a SISO system, from the input u, the state x and the measured output y, a general output predictor is written:

$$\hat{y}(t+1) = f_{nn}(y(t), \ldots, y(t-n_y), u(t), \ldots, (t-n_u),$$
$$x(t), \ldots, x(t-n_x)) \qquad (3)$$

The work presented here deals with the airpath control of SI engines. It is an extension of [7] which deals only with the turbocharger control. More precisely, it presents an up-to-date coordinated control scheme of all the air actuators: intake throttle, turbine wastegate and Variable Camshaft Timing (VCT). The control of dual equal VCTs has been studied in [8] and [9], but only in simulation, and is not completely detailed. [10] presented the control of dual equal VCT controllers, based on Hammerstein model. The coordination of the throttle and dual equal VCT has been studied in

[11]. The application treated here, the turbocharged SI engine with a twin independent VCT, is more complex, because the engine has more degrees of freedom. Moreover, it deals with high level variables which permit to control pollutant emissions, combustion stability, air scavenging, etc. . . , through a supervisor.

The control scheme proposed here combines separate, but coordinated, control modules for the different actuators. These modules are based on different model-based control strategies: Internal Model Control (IMC), Model Predictive Control (MPC), and optimal control. It is shown how neural models can be used at different levels and included in the control modules. The corresponding control principles are briefly recalled and the inclusion of neural models in such schemes is described. Particularly, it is shown how to include neural models in Nonlinear Model Predictive Control for such a fast system while ensuring low computational load. This is primarily obtained by instantaneous linearization and constraints holding by simple saturation.

In the next section, the air intake of a turbocharged SI engine, the control problem and the proposed torque control based on a coordinated control scheme of all the air actuators are presented. In the third section, the air mass control is described. First, the internal model control of the throttle, in which a neural model is used, is presented. Next, the wastegate control is described based on a Neural Predictive Control strategy. The air mass control has been tested on an engine test bench without Variable Camshaft Timing (VCT) and on a engine simulator with VCT [12]. In the fourth section, burned gas mass and scavenged air mass control is presented and the control of the Variable Camshaft Timing is described. It implements a neural model-based optimal control scheme, which consists of a minimization algorithm to be solved in real time. In this part, the controlled variable is not measured. This control has been tested on an engine test bench with VCT. All tests shown in this paper have been made on a test bench.

II. TURBOCHARGED SI ENGINE WITH VARIABLE CAMSHAFT ACTUATION

A. Air intake description

The air intake of a turbocharged SI Engine, represented in Figure 1, can be described as follows.

The compressor (pressure P_{int}) produces a flow from the ambient air (pressure P_{amb} and temperature T_{amb}). This air flow D_{thr} is adjusted by the intake throttle (section S_{thr}) and enters the intake manifold (pressure P_{man} and temperature T_{man}). The flow that goes into the cylinders D_{cyl} passes through the intake valves, whose timing is controlled by the intake Variable Camshaft Timing VCT_{in} actuator. After the combustion, the gases are expelled into the exhaust manifold through the exhaust valve, controlled by the exhaust Variable Camshaft Timing VCT_{exh} actuator. The exhaust flow is split in two parts: the turbine and wastegate flows. The turbine flow powers up the turbine and drives the compressor through a shaft. Thus, the supercharged pressure P_{int} is adjusted by the turbine flow which is controlled by the wastegate WG.
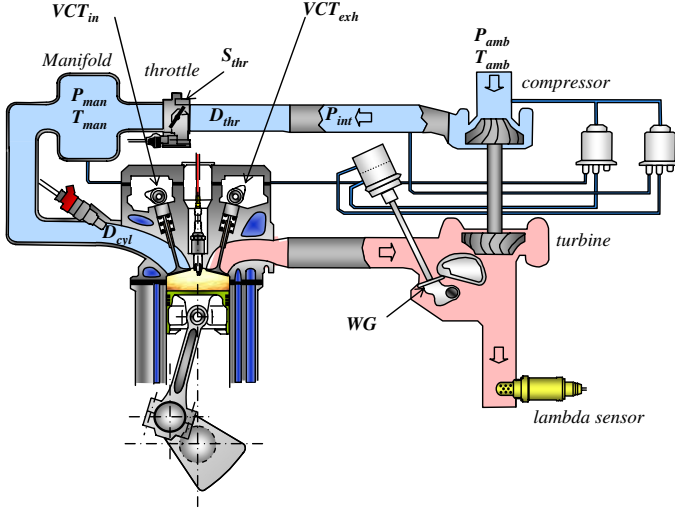
Fig. 1.   Airpath of a Turbocharged SI Engine with VCT

Fig. 2.   Proposed scheme for torque control

Fig. 3.   Proposed scheme for air actuator control

B. Torque control

The objective of engine control is to supply the torque requested by the driver while polluting the least amount as possible. For a SI engine, the torque is directly linked to the air mass trapped in the cylinder for a given engine speed N_e. For this reason, an efficient control of the air mass trapped in the cylinder is required to obtain the desired torque.

As the engine must pollute as little as possible, it is necessary to also control the back-flow of burned gases in the cylinder. Indeed, the residual burned gases in the cylinder reduce the pollutant formation (especially NO_x) because of the dilution, but the combustion stability and efficiency can be reduced as well. Thus an optimal value of burned gases in the cylinder must be tracked. The Recirculated Gas Mass RGM, that includes the burned gases, is controlled by the Variable Camshaft Timing (VCT).

The proposed torque control of the turbocharged SI engine with variable camshaft actuation is presented in Figure 2. The Torque Set Point is directly linked to the driver's request. The supervisor, not described in this paper, provides then two set points: the Air Mass Set Point M_{air_sp} and Recirculated Gas Mass Set Point RGM_{sp}, linked to pollutant emissions. The control is split into two parts: the air mass control, presented in more detail in part III, and the Recirculated Gas Mass control, detailed in part IV.

More precisely, as presented in Figure 3, the air mass control manipulates the throttle S_{thr} (block 2, section III-B) and the WasteGate WG (block 3, section III-C). It is necessary to compute beforehand a Manifold Pressure Set Point P_{man_sp} from the Air Mass Set Point M_{air_sp} (block 1, section III-A). Furthermore, the Recirculated Gas Mass control manipulates the Variable Camshaft Timing of the Intake VCT_{in} and of the Exhaust VCT_{exh} (block 4, section IV).

III.   AIR MASS CONTROL

A. From air mass to manifold pressure

This section corresponds to block 1 in Figure 3. To obtain the desired torque of a SI engine, the air mass trapped in
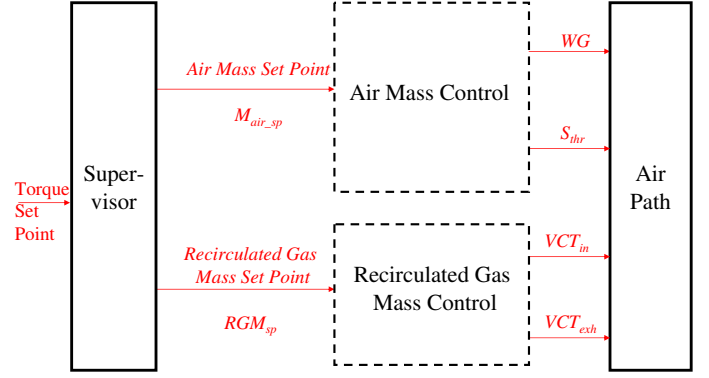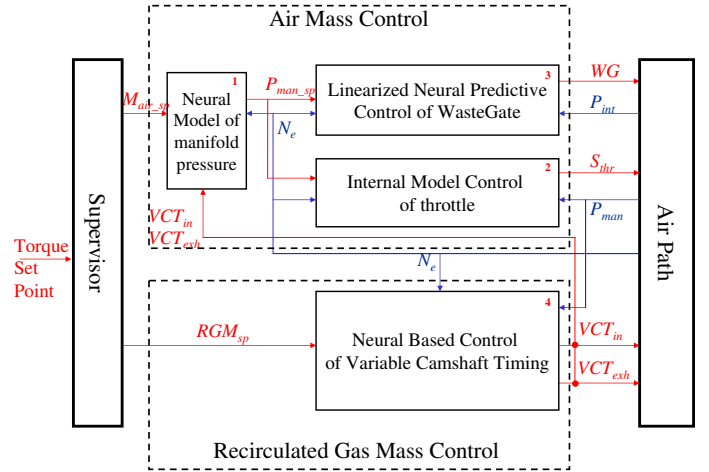
the cylinder must be precisely controlled. For an SI engine without Variable Camshaft Timing (VCT), the corresponding measurable variable is the manifold pressure, linearly related to the air mass trapped, as shown in Figure 4. Conversely, for an engine with Variable Camshaft Timing, there is no more one-to-one correspondence between the air mass trapped and the intake manifold pressure. Figure 4 also shows the relationship between the air mass trapped and the intake manifold pressure at two particular VCT positions for a fixed engine speed.

Thus, it is necessary to model the intake manifold pressure P_{man}. The static model chosen is a perceptron with one hidden layer (1). The regressors have been chosen from physical considerations: air mass M_{air} (corrected by the intake manifold temperature T_{man}), engine speed N_e, intake VCT_{in} and exhaust VCT_{exh} camshaft timing and then:

$$P_{man} = f_{nn1}\left(M_{air}, N_e, VCT_{in}, VCT_{exh}\right) \qquad (4)$$

The supervisor gives an air mass set point from the torque set point. From this air mass set point M_{air_sp}, the previous model gives the intake manifold pressure set point P_{man_sp}. So, the controlled variable is the intake manifold pressure P_{man}. The problem is therefore to manipulate the throttle S_{thr}
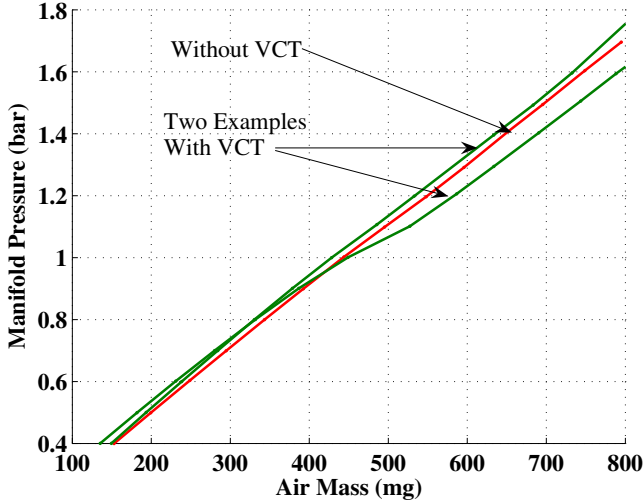
Fig. 4. Relationship between the manifold pressure (in bar) and the air mass trapped (in mg) for a SI Engine with VCT (green, two examples) and without VCT (red), at 2000 rpm

and the Wastegate WG to track the manifold pressure set point P_{man_sp}.

B. Intake throttle control

This section corresponds to block 2 in Figure 3.

1) Internal Model Control principle: The Internal Model Control (IMC) is a controller design strategy originally proposed for linear systems described by transfer function models [13], but extended to nonlinear systems [14] [15]. IMC has the following advantages: it is intuitively simple, easy to implement, and the only design parameter is for the filter. However, IMC can only be applied to stable processes. For unstable processes, a stabilizing feedback must be first carried out. Moreover, if the system has an unstable inverse, IMC cannot be applied. Due to the IMC structure, the integral action is implicitly included in the controller. In the linear case, one can prove that IMC allows to obtain the PID gains [16].
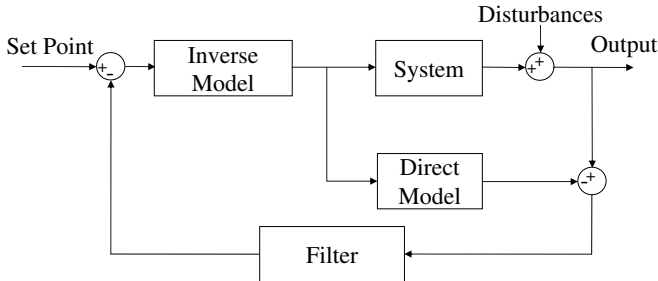

Fig. 5. Principle of Internal Model Control

Internal Model Control is based on the knowledge of a model of the process as shown in Figure 5. The internal models can be physical models or models identified from data. In the case where the direct model is perfect, the feedback signal is only the perturbation. Otherwise, the feedback signal includes the model error and some robustness

can be obtained by acting on a filter. This robustness filter can be a first order filter whose time constant is selected to ensure closed loop stability [14]. Moreover, if the steady-state gain of the inverse model is the inverse of the steady state gain of the direct model, a zero-offset is guaranteed.

2) Control scheme: The controlled variable is the intake manifold pressure P_{man} and the manipulated variable is the intake throttle S_{thr}.

a) Direct Model Description: The direct model used here is based on physical equations, as they present interesting characteristics: good extrapolation, good meaning, high reliability. This model is based on the perfect gas law:

$$P_{man}V_{man} = M_{man}RT_{man} \qquad (5)$$

with:
P_{man} intake manifold pressure (measured),
V_{man} manifold volume (known),
M_{man} intake manifold mass,
R perfect gases constant,
T_{man} intake manifold temperature (measured).

Differentiating this equation and considering a constant intake temperature (or slow variations) gives:

$$\dot{P}_{man} = \frac{RT_{man}(D_{thr} - D_{cyl})}{V_{man}} \qquad (6)$$

with:
D_{thr} flow through the throttle (in the manifold),
D_{cyl} flow through the intake valve (out the manifold).

On one hand, the flow through the throttle D_{thr} is calculated by the Barré de Saint-Venant equation [17]:

$$D_{thr} = S_{thr}P_{int}f(T_{man}, P_{man}/P_{int}) \qquad (7)$$

where:

$$\begin{cases} f(T, Pr) = \sqrt{\frac{2\gamma}{(\gamma-1)RT}\left(Pr^{\frac{2}{\gamma}} - Pr^{\frac{\gamma+1}{\gamma}}\right)} \\ \quad \text{if } Pr \geq (\frac{2}{\gamma+1})^{\frac{\gamma}{\gamma-1}} \simeq 0.5 \\ \\ f(T, Pr) = \sqrt{\frac{2\gamma}{(\gamma-1)RT}\left(\left(\frac{2}{\gamma+1}\right)^{\frac{2\gamma}{\gamma-1}} - \left(\frac{2}{\gamma+1}\right)^{\frac{\gamma+1}{\gamma-1}}\right)} \\ \quad \text{else} \end{cases}$$

$$(8)$$

with γ a thermodynamic constant.

On the other hand, the flow through the intake valve D_{cyl} is calculated by a classical volumetric efficiency technique:

$$D_{cyl} = \frac{n_{cyl}\eta_{vol}V_{cyl}P_{man}N_e}{120RT_{man}} \qquad (9)$$

with:
n_{cyl} number of cylinders (known),
η_{vol} volumetric efficiency,
V_{cyl} cylinder volume (known),
P_{man} intake manifold pressure (measured),
N_e engine speed (measured),
T_{man} intake manifold temperature (measured).

Without Variable Camshaft Timing, this volumetric efficiency η_{vol} is a function of the engine speed N_e and the intake manifold pressure P_{man}, practically given by a look-up table. With Variable Camshaft Timing, the intake VCT_{in} and exhaust VCT_{exh} Camshaft Timings have to be taken into account. So, a neural model is built:

$$\eta_{vol} = f_{nn2}\left(P_{man}, N_e, VCT_{in}, VCT_{exh}\right) \qquad (10)$$

b) Inverse Model Description: The inverse model can be a static model [13]. Here, the static inverse model is given by considering $\dot{P}_{man} = 0$ in (6). This gives simply:

$$D_{thr} = D_{cyl} \qquad (11)$$

and then, with (7):

$$S_{thr} = \frac{D_{cyl}}{P_{int} f(T_{man}, P_{man}/P_{int})} \qquad (12)$$

As the direct and the inverse models are derived from the same equations, the steady state gain of the inverse model is the inverse of the steady state gain of the direct model. Consequently, a zero-offset is guaranteed.

The Internal Model Control of the throttle is summarized in Figure 6. The direct model is given, after discretization, by (6), with (7), (8), and (9), and the inverse model by (12), with (8) and (9). For both direct and inverse models, the volumetric efficiency can be given by a lookup-table $\eta_{vol} = f(N_e, P_{man})$ without VCT, or the neural model (10) with VCT. Variables P_{int}, T_{man} and N_e are measured.
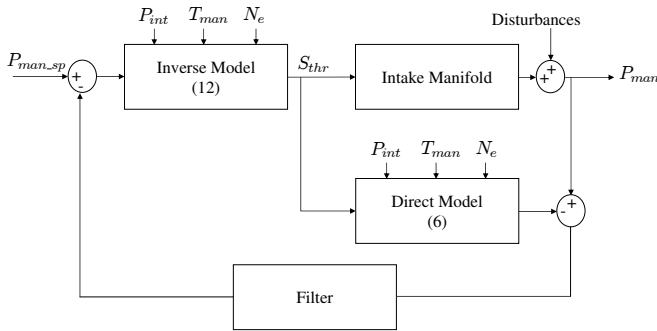

Fig. 6.   Internal Model Control of the throttle

3) Engine test bench results: IMC was compared to a classical feedforward control scheme based on (12) plus a PID controller. Figure 7 shows the results obtained on a 0.6 Liter turbocharged 3 cylinders *Smart* engine (without Variable Camshaft Timing). The IMC results are clearly better. But the main advantage of IMC is the easy synthesis and tuning of the control.

C. WasteGate control

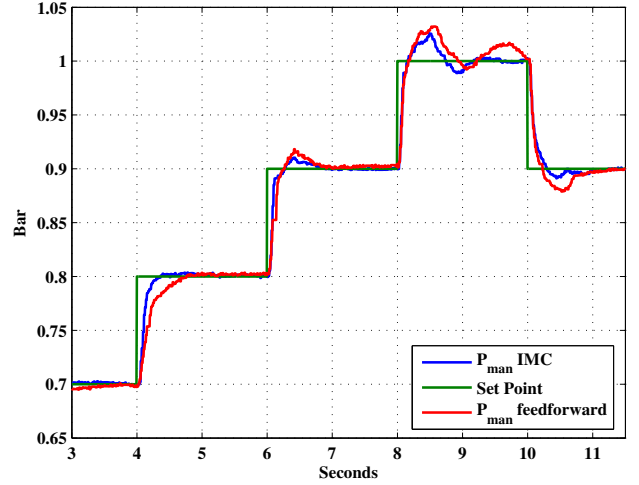This section corresponds to block 3 in Figure 3.

Fig. 7.   Intake Manifold Pressure P_{man} (bar): setpoint, variable controlled by feedforward control ($P_{man} feedforward$) and Internal Model Control ($P_{man} IMC$). Results obtained on test bench

1) Principle of Model Predictive Control: Model Predictive Control (MPC) or Receding Horizon Control (RHC) has become an attractive control strategy especially for linear processes or nonlinear processes with large time constant. MPC uses an explicit model to predict the future response of the process and an algorithm optimizing the future process behavior. In general, MPC is formulated as solving on-line, at each sampling instant, a finite horizon open-loop optimal control problem subject to system dynamics and constraints involving states and controls [18]. The optimization produces an optimal control sequence and only the first value in this sequence is applied to the process.

Linear Model Predictive Control deals with old and intuitive ideas, but has only expanded more rapidly in the 1980's. Linear MPC uses a linear model to predict the process behavior, so that the solution or a part of the solution can be calculated off line. For a good introduction to the theoretical and practical issues associated to linear MPC, see [19], [20], and [21]. Many systems are, however, nonlinear by nature, and linear models are often inadequate to describe such processes. This motivates the development of Nonlinear Model Predictive Control (NMPC) [22]. Due to the use of a nonlinear model, NMPC strategy is based on solving a non-convex optimization problem on-line, which requires an important computational load. If neural models are associated in the NMPC strategy, the control scheme is called Neural Predictive Control [23].

Model Predictive Control, illustrated for a SISO system in Figure 8, unfolds in three steps. The first step is the prediction of the output on a horizon T_p from inputs (present and future) and measured outputs. This prediction can be made by a physical model or an identified model which can be linear or not. The second step consists in simulating the output set point y_{sp} on the same horizon T_p with a reference model. To allow a soft attenuation of the error, a first order exponential trajectory could be chosen:
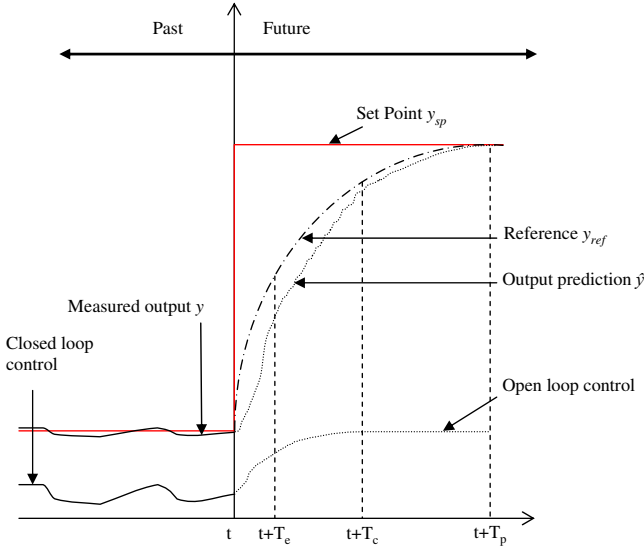
Fig. 8. Principle of Model Predictive Control

$$y_{ref}(t+i) = y(t) + [y_{sp}(t) - y(t)] \left(1 - e^{-\frac{iT_e}{\tau}}\right) \quad (13)$$

with:

τ	time constant of the desired transient,
y	measured process output,
y_{sp}	output set point,
T_e	sampling period.

The last step consists of the minimization over a finite horizon of a (most often) quadratic performance index J:

$$J = \sum_{i=1}^{m} \left(\sum_{j=1}^{T_{pi}} [(y_{iref}(t+j) - \hat{y}_i(t+j)]^2 \right) \\ + \sum_{i=1}^{n} \left(\rho_i \sum_{j=0}^{T_c} [u_i(t+j) - u_i(t+j-1)]^2 \right) \quad (14)$$

with respect to the control vector:

$$\underline{U} = [u_1(t) \ldots u_n(t); \ldots ; u_1(t+T_c) \ldots u_n(t+T_c)] \quad (15)$$

subject to the constraint $\underline{U} \in D$

with:

n,m	number of inputs and outputs,
T_{pi}	i^{th} prediction horizon,
T_c	control horizon,
y_{iref}	reference for the ith output,
$\hat{y}_i$	i^{th} predicted output,
ρ_i	weighting factors,
D	variation domain of the control.

Only the first control vector $[u_1(t) \ldots u_n(t)]$ is applied to the process.

Real time requirement is an important problem for practical control systems especially with NMPC. All the iterative min-imizations must be solved on-line at each step which requires intensive computations. Very few works deal with real-time implementation of NMPC [24] or the works are applied to plants that have a large time constants [23]. For real-time implementation, a solution for the optimization problem is needed which should not be an intensive iterative procedure. Furthermore, the available optimization algorithms cannot guarantee that the solution can be obtained in guaranteed time and that the solution obtained is a global minimum. These problems can be partially overcome by instantaneous linearisation.

The local linearization of a particular form of (3):

$$\hat{y}(t+1) = f_{nn}\left(y(t), u(t), x(t)\right) \quad (16)$$

around an operating point y_0, x_0 and u_0 gives:

$$\hat{y}(t+1) = a_0 + b_0 y(t) + c_0 u(t) \quad (17)$$

with:

$$a_0 = f_{nn}|_0 - \left.\frac{\partial f_{nn}}{\partial y(t)}\right|_0 y_0 - \left.\frac{\partial f_{nn}}{\partial u(t)}\right|_0 u_0 \\ b_0 = \left.\frac{\partial f_{nn}}{\partial y(t)}\right|_0 \\ c_0 = \left.\frac{\partial f_{nn}}{\partial u(t)}\right|_0 \quad (18)$$

For sake of clarity, the changes on the states $x(t)$ around x_0 have been assumed to be sufficiently small. In a matrix form, for a SISO system, the prediction vector with $T_c = T_p - 1$ is given by:

$$\hat{Y} = G + HU \quad (19)$$

with:

$$\hat{Y} = [\hat{y}(t+1) \cdots \hat{y}(t+T_p)]^T \\ U = [u(t) \cdots u(t+T_p-1)]^T \quad (20)$$

$$H = \begin{bmatrix} c_0 & 0 & \cdots & 0 \\ b_0 c_0 & c_0 & \ddots & \vdots \\ \vdots & \ddots & \ddots & 0 \\ b_0^{T_p-1} c_0 & \cdots & b_0 c_0 & c_0 \end{bmatrix} \quad (21)$$

$$G = \begin{bmatrix} a_0 + b_0 y(t) \\ a_0 + a_0 b_0 + b_0^2 y(t) \\ \vdots \\ a_0 \sum_{j=0}^{T_p-1} b_0^j + b_0^{T_p} y(t) \end{bmatrix} \quad (22)$$

The performance index (14) can be thus written:

$$J = \left(\hat{Y} - Y_{ref}\right)^T \left(\hat{Y} - Y_{ref}\right) + \left(U^T \Gamma U - 2\beta^T U + r\right) \quad (23)$$

with:

$$Y_{ref} = [y_{ref}(t+1) \cdots y_{ref}(t+T_p)]^T$$

$$\Gamma = \rho \begin{bmatrix} 2 & -1 & & 0 \\ -1 & \ddots & \ddots & \\ & \ddots & 2 & -1 \\ 0 & & -1 & 1 \end{bmatrix}, \beta = \rho \begin{bmatrix} u_0 \\ 0 \\ \vdots \\ 0 \end{bmatrix}, r = \rho u_0^2 \quad (24)$$

Then, the minimization problem can be written:

$$\min_{U \in D} \frac{1}{2} U^T \left(H^T H + \Gamma \right) U + \left((G - Y_{ref})^T H - \beta^T \right) U \quad (25)$$

To deal with the constraint, two solutions can be used. The first one is an iterative procedure for the constrained minimization. In the second one, the control is the saturated solution of the unconstrained minimization so that an analytical solution is found:

$$U = \text{sat} \left\{ \left(H^T H + \Gamma \right)^{-1} \left(\beta - H^T (G - Y_{ref}) \right) \right\} \quad (26)$$

This control scheme, which guarantees a satisfactory computational burden, is called here the Saturated Linearized Neural Predictive Control (SLNPC) [7].

2) Control scheme: The torque set point is rewritten into a Air Mass Set Point M_{air_sp} that gives the manifold Pressure set point P_{man_sp} (see section III-A). If the manifold pressure is less than the ambient pressure ($P_{man\_sp} < P_{amb}$), the WasteGate is opened ($WG = 0$), and the manifold pressure is controlled by the throttle (see section III-B). But if the manifold pressure is greater than the ambient pressure ($P_{man\_sp} > P_{amb}$), there is an infinite number of solutions for actuators opening (S_{thr} and WG), but only one is optimal from the efficiency point of view. To maximize the efficiency, i.e. to reduce the pumping losses [17], the throttle should be wide open. It is worth noting that throttle is opened when $P_{int} \approx P_{man}$, and thus the supercharging pressure target is the same as the manifold pressure target P_{man_sp}.

In summary, the controlled variable is here the supercharging pressure P_{int} and the manipulated variable is the wastegate WG. Moreover the WasteGate control is multiobjective: to have the maximum opening of the throttle S_{thr} and to track the intake manifold pressure set point P_{man_sp}.

a) Prediction Model: A Linear Model Predictive Controller would give bad results because of the static nonlinearities shown in Figure 9. It can be noticed that these nonlinearities, given at a fixed engine speed N_e, look like sigmoïdal functions.

A neural black-box predictor of P_{int} is used because the corresponding physical model of the turbocharger is poor and too complex to be embedded and differentiated, in the MPC framework. The neural model is trained from test bench data (but can be learned on a simulator too). The learning data base has been built so that there is no gap in the frequency and amplitude domains. Based on physical considerations, the following regressors have been chosen: $P_{int}(t)$, $WG(t)$, the wastegate closing, and $D_{cyl}(t)$, the air mass flow entering the
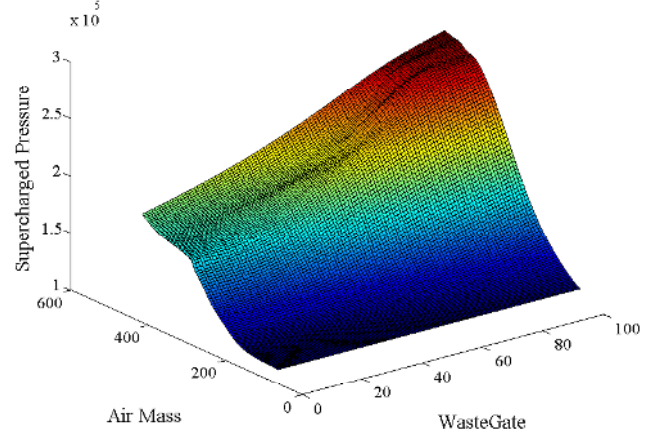

Fig. 9. Static Non Linearities of the supercharged pressure (Pascal) versus WasteGate closing (%) and Air Mass (mg) at a fixed engine speed $N_e = 3000$ rpm

cylinders obtained by an estimator given by (9). This air mass flow $D_{cyl}(t)$ is chosen because it is an image of the engine load and takes into account the Variable Valve Actuation. The model is then given by:

$$\hat{P}_{int}(t+1) = f_{nn3}\left(P_{int}(t), WG(t), D_{cyl}(t)\right) \quad (27)$$

where f_{nn3} is a one hidden layer perceptron with 5 neurons and with a sampling period of 0.03 s. The training signals have been collected on the same 0.6 Liter turbocharged 3 cylinders *Smart* engine and then scaled. To train the neural model, steps of wastegate and throttle are applied with the same range of the test signals. These steps are generated by an Amplitude modulated Pseudo Random Binary Sequence (APRBS) [25] for various engine speeds (1500, 2000, 2500, 3000 and 3500 rpm). It is worth noting that only 200 seconds are necessary to collect the data (for each engine speed). Training has been performed by minimizing the mean squared error, using the Levenberg-Marquardt algorithm [26]. The model validation is illustrated in Figures 10 and 11. Figure 10 shows the estimation error and the very good prediction given by the neural model overwritten by the actual value of P_{int}. Figure 11 shows the responses of the actuators for the same test. For that test, the autocorrelation function of the prediction error is satisfying as shown in figure 12 so that the model is accepted.

b) Performance Index: The performance index of the Neural MPC applied to the turbocharged SI engine is given by:

$$J = \begin{array}{l} \sum_{j=1}^{T_p} [(P_{intref}(t+j) - \hat{P}_{int}(t+j)]^2 \\ + \rho \sum_{j=0}^{T_p-1} [WG(t+j) - WG(t+j-1)]^2 \end{array} \quad (28)$$

where the prediction horizon is set according to the system dynamics ($T_p = 3$). The weight factor ρ is set to 5e-2 (after normalizing) to reach a good compromise between fast
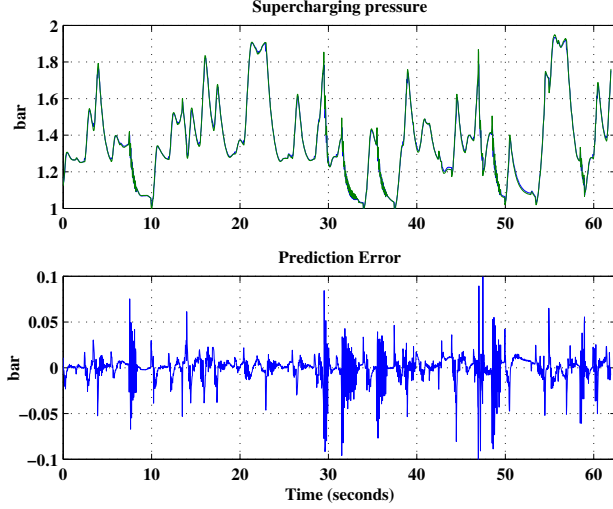
Fig. 10. Real and predicted supercharging pressure (bar) (top) and estimation error (bottom) versus time (seconds) for the test. Results obtained on test bench
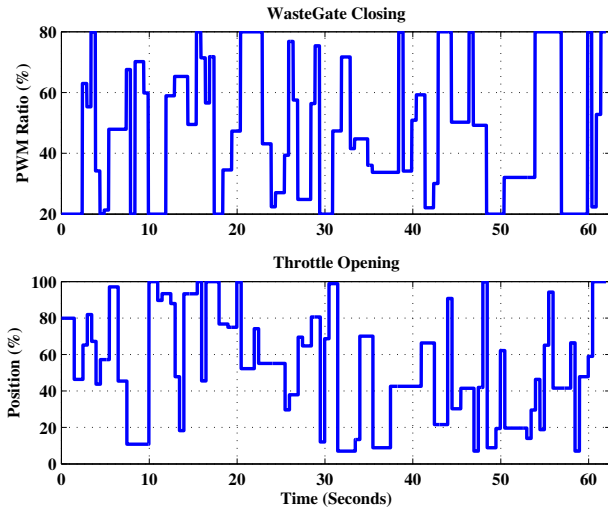

Fig. 11. Wastegate closing (PWM ratio, %) (top) and throttle opening (position, %) (bottom) versus time (seconds) for the test. Results obtained on test bench
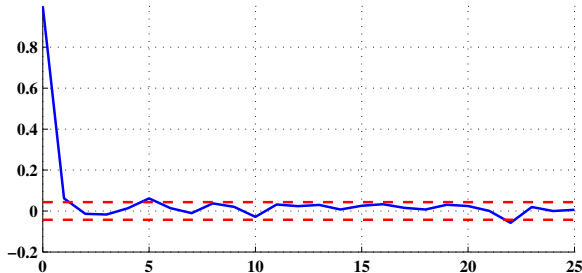

Fig. 12. Autocorrelation function of the prediction error versus lag

system response and low actuator solicitation. The reference model is given by (13) where the time constant is fixed to 0.05 s. The target of the supercharging pressure (P_{int}) is the same as the target of the manifold pressure (P_{man}) so that the throttle is opened as wide as possible.

3) Engine test bench results: Some results of the *Saturated Linearized Neural Predictive Control* (14), for the same engine test bench, are displayed in Figures 13 and 14. Figure 13 shows the manifold pressure set point, the supercharging pressure (which cannot be less than $P_{amb} \approx 1$bar) and the manifold pressure when the torque target changes. Figure 14 shows the actuators response during the same test. The chosen engine speed (2750 rpm) is not included in the training data of the supercharging pressure P_{int}. Various engine speeds were tested with nearly the same results. This shows the good control performances of the proposed method. Note that the throttle is opened as wide as possible, because $P_{int} \approx P_{man}$, so that the objectives are satisfied.
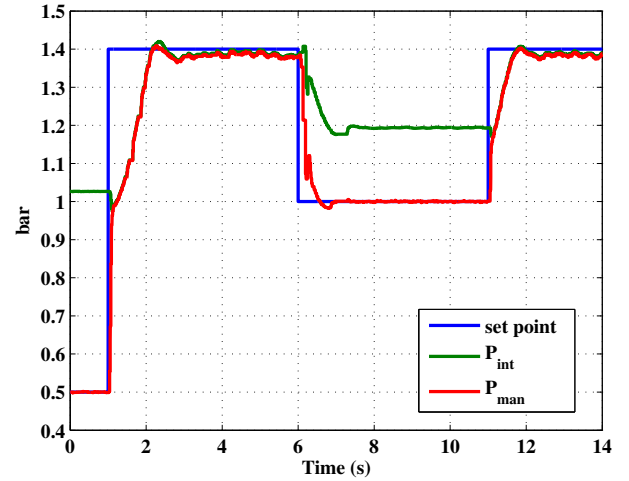
Fig. 13. Pressures (bar) versus time (seconds): setpoint, supercharged pressure P_{int}, intake manifold pressure P_{man}, at N_e=2750 rpm. Results obtained on test bench

The torque control is split in two parts as shown in Figure 2. The air mass control has been described in this section. The Recirculated Gas Mass control is presented below.

IV. RECIRCULATED GAS MASS CONTROL

This section corresponds to block 4 in Figure 3.

A. Neural model of the Recirculated Gas Mass

The effects of Variable Camshaft Timing (VCT) can be summarized as follows. On the one hand, cam timing can inhibit the production of nitrogen oxides (NO_x) because of the in-cylinder burned gases. Indeed, by acting on the cam timing, combustion products which would otherwise be expelled during the exhaust stroke are retained in the cylinder during the subsequent intake stroke. This dilution of the mixture in the cylinder reduces the combustion temperature and limits
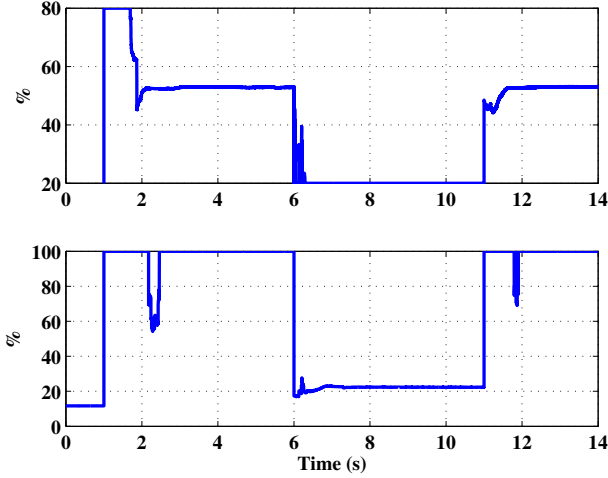
Fig. 14. Wastegate closing (PWM ratio, %) (top) and throttle opening (position, %) (bottom) at 2750 rpm. Results obtained on test bench

Fig. 15. Recirculated Gas Mass at $N_e = 2000$ rpm and $P_{man} = 1.4$ bar

the NO_x formation. Therefore, it is important to control the burned gas back-flow in the cylinder.

On the other hand, with camshaft timing, air scavenging can appear, that is air passing directly from the intake to the exhaust through the cylinder. For that, the intake manifold pressure must be greater than the exhaust pressure when the exhaust and intake valves are opened together. In that case, the turbocharger and engine torque dynamic behavior are improved (the response times are decreased). Indeed, the flow which passes through the turbine is increased and the energy retrieved by the turbine is given to the compressor. In transient, it is very important to control this scavenging.

Because scavenging and burned gas back-flow correspond to the same flow phenomenon, only one variable, noted here as RGM (Recirculated Gas Mass), is necessary:

$$RGM = \begin{cases} M_{burned\ gas} & \text{if } M_{burned\ gas} > M_{scavenged} \\ -M_{scavenged} & \text{else} \end{cases}$$
(29)

Note that, when there is scavenging from the intake to the exhaust, the burned gases are insignificant. Figure 15 shows the Recirculated Gas Mass RGM on an operating point, i.e. at a fixed engine speed and a fixed manifold pressure.

Studying this variable is complex because it cannot be measured on-line (or the measurement is too complex). To control RGM, the only method is to build a model from a complex but accurate high frequency simulator. A static neural model has been chosen:

$$\widehat{RGM} = f_{nn4}(P_{man}, N_e, VCT_{in}, VCT_{exh})$$
(30)

with:

$\widehat{RGM}$	Recirculated Gas Mass observation,
P_{man}	intake manifold pressure,
N_e	engine speed,
VCT_{in}	intake camshaft timing,
VCT_{exh}	exhaust camshaft timing.

The choice of the regressors is based on physical considerations. The learning bases (about 6800 points) comprises all the representative static operating points : manifold pressure from 0.3 bar to 2.4 bar, engine speed from 750 rpm to 5500 rpm, intake camshaft timing and exhaust camshaft timing from 0 to 40^oCA (crankshaft angle degree).

B. Control scheme

The controlled variable is the non-measured variable $\widehat{RGM}$ and the manipulated variables are the intake Variable Camshaft Timing (VCT_{in}) and the exhaust Variable Camshaft Timing (VCT_{ech}). A feedforward control scheme based on an inverse model cannot be applied, because the system is not bijective as shown in figure 15. Thus, the burned gas control consists of a neural model-based scheme solving in real time the following minimization:

$$\min_{\substack{0 \leq VCT_{in} \leq 40 \\ 0 \leq VCT_{exh} \leq 40}} J$$
(31)

with:

$$J = \begin{array}{l} \left(\widehat{RGM} - RGM_{sp}\right)^2 \\ + \rho_1(\Delta VCT_{in})^2 + \rho_2(\Delta VCT_{exh})^2 \end{array}$$
(32)

$\widehat{RGM}$	Recirculated Gas Mass observation,
RGM_{sp}	Recirculated Gas Mass set point,
ΔVCT_{in}	intake camshaft timing variation,
ΔVCT_{exh}	exhaust camshaft timing variation,
ρ_1, ρ_2	weighting factors.

Many options are available for this minimization [25]. The chosen method is a full-Newton Levenberg-Marquardt method [23]. The advantage of a such method is the convergence and the computational aspect for small order systems. The minimization of the performance index J (32) with respect to the control vector $VCT = [VCT_{in}, VCT_{exh}]$ can be written in ten steps:
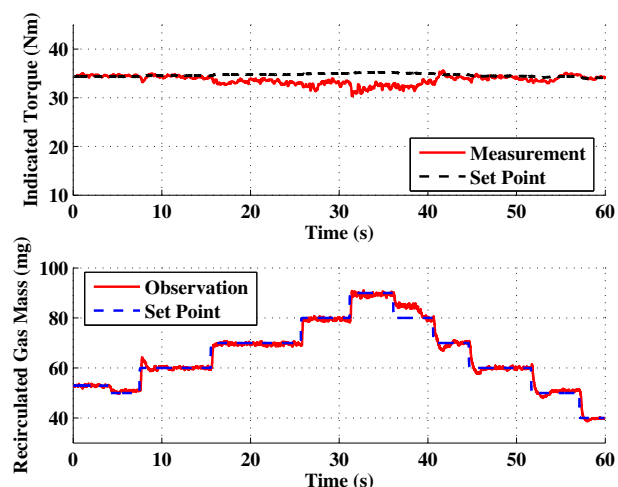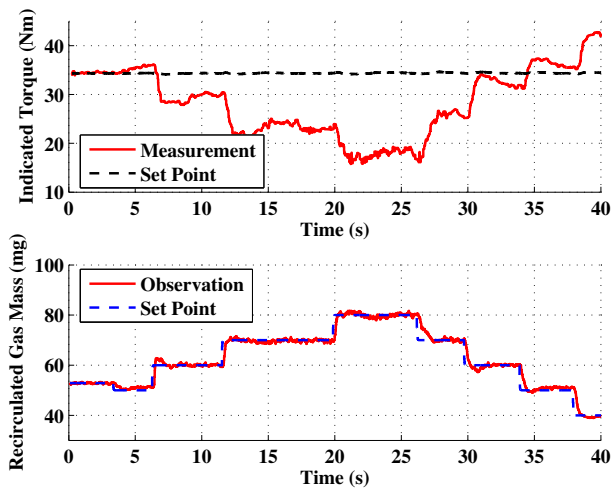
Fig. 19. Effect of the Recirculated Gas Mass (mg, bottom) on the Indicated Torque (Nm, top) without the proposed control scheme

V. CONCLUSION

This paper has presented the inclusion of neural models in various automotive engine control schemes. The proposed approach has been tested on a up-to-date nonlinear fast coupled system, the air intake control of a turbocharged SI engine with the aim of downsizing. The control scheme, tested on two different engine test benches for various engine speeds, uses three controllers: the throttle controller, the wastegate controller, and the VCT controller. Instead of using a complex unique controller, the idea is to combine separate, but coordinated, control modules that are easier to synthesize, to implement and to tune.

The Internal Model Control of the throttle is mainly based on a first principle model. The wastegate control is a Model Predictive Control where a neural model is used as nonlinear predictor. The proposed method, linearized neural predictive control, guarantees the application to fast time constant nonlinear systems. The Variable Camshaft Timing control uses a model-based control scheme where a neural model gives an observation of a non measured variable. In these cases, neural networks are used to replace physical models, which are too complex to be on line embedded.

The good control performances of the proposed methods were demonstrated on two engine test benches. While a part of the work presented here has been tested on a test bench without Variable Camshaft Timing (for the wastegate and the throttle), further work will be to apply the complete control scheme to an engine bench with Variable Camshaft Timing. Finally, further research will deal with the supervisor synthesis.

ACKNOWLEDGMENT

REFERENCES

[1] B. Lecointe and G. Monnier, "Downsizing a gasoline engine using turbocharging with direct injection," *SAE Technical Papers*, no. 2003-01-0542, 2003.

[2] G. Corde, "Le contrôle moteur," in *Contrôle commande de la voiture*, G. Gissinger and N. Le Fort Piat, Eds. Hermès, 2002.

[3] J. Sjöberg, Q. Zhang, L. Ljung, A. Benveniste, B. Delyon, P. Glorennec, H. Hjalmarsson, and A. Juditsky, "Nonlinear black-box modeling in system identification: a unified overview," *Automatica*, vol. 31, no. 12, pp. 1691–1724, 1995.

[4] G. V. Puskorius, L. Feldkamp, and L. Davis, "Dynamic neural methods applied to on-vehicle idle speed control," in *Proc. of the IEEE*, vol. 84, October 1996, pp. 1407–1419.

[5] C. Alippi, C. de Russis, and V. Piuri, "A neural-network based control solution to air-fuel ratio control for automotive fuel-injection systems," *IEEE Trans. on Systems, Man, and Cybernetics - Part C: Applications and Reviews*, vol. 33, no. 2, pp. 259–268, 2003.

[6] M. Beham, , and D. Yu, "Modeling a variable valve timing spark ignition engine using different neural networks," *Proc. Instn Mech. Engrs*, vol. 218, pp. 1159–1171, 2004.

[7] G. Colin, Y. Chamaillard, G. Bloch, G. Corde, and A. Charlet, "Linearized neural predictive control. A turbocharged SI engine application," *SAE 2005 Transactions Journal of Engines*, pp. 101–108, SAE Technical Paper 2005–01–046, 2005.

[8] A. Stephanopoulou, J. Cook, J. Freudenberg, J. Grizzle, M. Haghgooie, and P. Szpak, "Modelling and control a spark ignition engine with variable cam timing," in *Proc. of the American Control Conference*, Seattle, 1995, pp. 2576–2581.

[9] J. C. D. Gorinevsky and G. Vukovich, "Nonlinear predictive control of transients in automotive variable cam timing engine using nonlinear parametric approximation," *Journal of Dynamic Systems, Measurement and Control*, vol. 125, pp. 429–438, 2003.

[10] A. Stefanopoulou and I. Kolmanovsky, "Analysis and control of transient torque response in engines with internal exhaust gas recirculation," *IEEE Transactions on Control Systems Technology*, vol. 7, no. 5, pp. 555–565, 1999.

[11] M. Jankovic, "Nonlinear control in automotive engine applications," in *Electronic Proceedings of the 15th Int. Symp. on the Mathematical Theory of Networks and Systems*, University of Notre Dame, USA, 2002.

[12] A. Albrecht, G. Corde, V. Knop, H. Boie, and M. Castagne, "1D simulation of turbocharged gasoline direct injection engine for transient strategy optimization," *SAE Technical Papers*, no. 2005-01-0693, 2005.

[13] P. De Larminat, *Commande des systèmes linéaires*. Paris: Hermès, 1993.

[14] C. Economou, M. Morari, and B. Palsson, "Internal Model Control 5. Extensions to Nonlinear Systems," *Ind. Eng. Process Des. Dev*, vol. 25, pp. 403–411, July 1986.

[15] M. Henson and D. Seborg, "An Internal Model Control Strategy for Nonlinear Systems," *AIChE Journal*, vol. 37, no. 7, pp. 1065–1081, July 1991.

[16] J. Corriou, *Process Control - Theory and applications*. Springer, 2004.

[17] J. Heywood, *Internal Combustion Engine Fundamentals*. McGraw-Hill, 1988.

[18] D. Clarke, C. Mohtadi, and P. Tuffs, "Generalized Predictive Control - part I. the basic algorithm," *Automatica*, vol. 23, pp. 137–148, 1987.

[19] C. Garcia, D. Prett, and M. Morari, "Model Predictive Control : theory and practice - a survey," *Automatica*, vol. 25, no. 3, pp. 335–348, 1989.

[20] M. Morari and J. Lee, "Model Predictive Control : past, present, future," *Computers and Chemical Engineering*, vol. 23, pp. 667–682, 1999.

[21] S. Qin and T. Badgwell, "A survey of industrial model predictive technology," *Control Engineering and Practice*, vol. 11, pp. 733–764, 2003.

[22] R. Findeisen and C. Allgower, "An introduction to Nonlinear Model Predictive Control," in *21st Benelux Meeting on systems and control*, The Netherlands, March 2002.

[23] M. Norgaard, O. Ravn, N. Poulsen, and L. Hansen, *Neural Networks for Modeling and Control of Dynamics Systems*. Springer, 2000.

[24] P. Haley, D. Soloway, and B. Gold, "Real time adaptative control using Neural Generalized Predictive Control," in *Proc. of the American Control Conference*, San Diego, CA, 1999.

[25] O. Nelles, *Nonlinear System Identification*. Springer, 2000.

[26] M. Norgaard, "Neural network based system identification toolbox," Department of Automation, Technical University of Denmark, Tech. Rep. 00-E-891, 2000.